E-ISSN: 3123-2574
DOI: https://doi.org/10.64803/ikosstemi.v2.152 | Page: 18-24

Spatial Data Analysis for Environmental and Climate Monitoring Using Google Earth Engine and Random Forest Classification

Supiyandi[1,2], Ramlah binti Mailok[2*]
[1,2]Faculty of Computing and META Technology Information System and Management, Universiti Pendidikan Sultan Idris, Tanjong Malim, Perak, Malaysia
[1]Faculty of Computational Science and Digital Intelligence, Information Technology, Universitas Pembangunan Panca Budi, Medan, Indonesia
E-mail: [1]supiyandiyt@gmail.com, [2*]mramlah@meta.upsi.edu.my
*E-mail Corresponding Author: mramlah@meta.upsi.edu.my

Abstract

Land-cover change is a primary driver of environmental degradation and local climate alteration, yet up-to-date, spatially explicit information remains scarce in rapidly developing regions such as North Sumatra, Indonesia. This study aims to develop an accurate, reproducible workflow for environmental and climate monitoring by integrating cloud-based spatial data processing with machine-learning classification. Multitemporal Sentinel-2 surface-reflectance imagery (2019 and 2024) and Landsat-derived land-surface temperature were processed on the Google Earth Engine (GEE) platform. Spectral bands were combined with vegetation, water, and built-up indices (NDVI, NDWI, NDBI, EVI, SAVI, BSI) and topographic data, after which a Random Forest (RF) classifier distinguished six land-cover classes from stratified training samples. The RF model achieved an overall accuracy of 92.4% and a kappa coefficient of 0.906, outperforming Classification and Regression Tree (86.1%) and Support Vector Machine (88.7%) baselines. NDVI, the near-infrared band, and NDWI were the most influential predictors. Between 2019 and 2024 the built-up area expanded by 18.7% while forest and cropland contracted, and these changes coincided with a measurable rise in land-surface temperature, confirming a strong inverse relationship between vegetation cover and surface heating. The results demonstrate that the GEE–RF approach provides a low-cost, scalable, and replicable basis for routine environmental and climate monitoring to support evidence-based regional planning.

Keywords: *Google Earth Engine; Random Forest; land-cover classification; Sentinel-2; climate monitoring*

I. INTRODUCTION

Environmental degradation and local climate change are among the most pressing challenges facing developing regions. Rapid urbanisation, agricultural expansion, and deforestation continuously reshape the Earth surface and alter the exchange of energy and moisture between land and atmosphere. In North Sumatra, Indonesia, the Medan metropolitan area and its surrounding districts have experienced sustained built-up expansion over the past decade, accompanied by the conversion of vegetated land into impervious surfaces. According to national statistics, urban land in the province has grown by more than 15% since 2015, intensifying surface runoff, biodiversity loss, and the urban heat-island effect. Reliable, spatially explicit, and frequently updated land-cover information is therefore essential for diagnosing these pressures and guiding mitigation policy.

North Sumatra exemplifies these pressures. The province combines a fast-growing metropolitan core with extensive lowland agriculture, oil-palm estates, and remnant forest, and it has experienced recurrent flooding, riverbank erosion, and heat stress that are widely attributed to vegetation loss and impervious-surface expansion. Mapping and monitoring such a heterogeneous landscape demands data that are both spatially detailed and temporally repeatable, yet field surveys are costly and infrequent. Satellite remote sensing, processed in the cloud, offers the only practical means of producing consistent, wall-to-wall information at the cadence that planning agencies require.

Conventional land-cover mapping based on the manual download and desktop processing of satellite scenes is time-consuming, storage-intensive, and difficult to repeat across large areas or long time series. The emergence of cloud-based geospatial platforms has transformed this situation. Google Earth Engine (GEE) provides petabyte-scale access to multi-sensor archives together with distributed processing, enabling analysts to compose, filter, and classify imagery without local downloads (Gorelick et al., 2017). Recent reviews confirm that GEE has become a dominant environment for remote-sensing big-data applications, including land-cover mapping, change detection, and climate monitoring (Amani et al., 2020; Tamiminia et al., 2020). Nevertheless, many regional studies still rely on a single sensor or a single date, which limits the separability of spectrally similar classes and weakens the robustness of derived change statistics.

Among the classifiers available on these platforms, the Random Forest (RF) algorithm has consistently demonstrated strong performance for land-cover classification. As an ensemble of decision trees trained on bootstrapped samples and random feature subsets, RF is robust to noise, handles high-dimensional inputs, and provides an internal measure of variable importance (Breiman, 2001; Belgiu & Dragut, 2016). Comparative experiments report that RF generally matches or exceeds Support Vector Machine and decision-tree classifiers when applied to Sentinel-2 imagery (Thanh Noi & Kappas, 2018; Phan et al., 2020), and machine-learning classifiers more broadly have become the standard for satellite-based land-use and land-cover mapping (Talukdar et al., 2020). The combination of GEE and RF has been applied successfully across agricultural, forest, and urban settings (Habibie, 2022; Ouchra et al., 2024; Tassi & Vizzari, 2020).

Land-cover information also underpins climate monitoring at the local scale. Land-surface temperature, retrievable from the thermal infrared bands of Landsat sensors, is a sensitive indicator of how surface composition modulates the energy balance. Vegetation cools the surface through evapotranspiration and shading, whereas impervious materials store and re-emit heat, producing the surface urban heat-island effect. By utilising the Normalised Difference Vegetation Index (NDVI) and Google Earth Engine (GEE) and Sentinel-2 satellite images, this research aims to develop and evaluate a model for predicting urban vegetation cover in Batu Bara Regency, Indonesia (Supiyandi & R. b. Mailok, 2025). Because vegetation indices such as NDVI and surface temperature are physically linked, combining a land-cover classification with an LST layer enables analysts not only to map what is on the ground but also to quantify the thermal consequences of land conversion—an integration that remains uncommon in regional remote-sensing studies of Indonesia.

Despite this progress, comparatively few studies integrate spectral classification with an explicit climate variable such as land-surface temperature (LST) within a single reproducible GEE workflow, and even fewer focus on the rapidly changing landscape of North Sumatra. The objective of this study is therefore to build and evaluate a GEE-based pipeline that couples multitemporal Sentinel-2 imagery and RF classification with LST analysis to monitor environmental and climate change between 2019 and 2024. The study contributes (i) a transferable feature set combining spectral bands, indices, topography, and LST; (ii) a quantitative accuracy benchmark of RF against CART and SVM; and (iii) an interpretation of how observed land-cover change relates to local surface warming, addressing the gap between land-cover mapping and climate-impact assessment.

II. RESEARCH METHODOLOGY

The research adopts a quantitative, supervised-classification design implemented entirely on the Google Earth Engine cloud platform. The overall workflow, summarised in Figure 1, proceeds from image acquisition and preprocessing, through feature engineering and sample collection, to Random Forest classification, accuracy assessment, and change analysis.

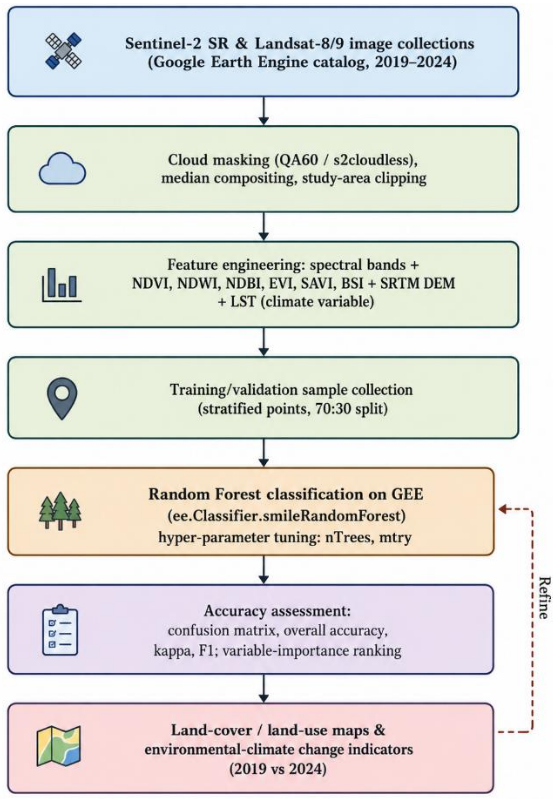

Figure 1. Research framework of the Google Earth Engine and Random Forest land-cover classification workflow.

The study area covers the Medan–Deli Serdang corridor in North Sumatra, Indonesia, a mixed

E-ISSN: 3123-2574
DOI: https://doi.org/10.64803/ikosstemi.v2.152 | Page: 18-24

landscape of urban settlement, oil-palm and food-crop agriculture, secondary forest, and river systems. Sentinel-2 Level-2A surface-reflectance image collections were used as the primary data source for the dry-season windows of 2019 and 2024, while Landsat-8/9 Collection-2 thermal data supplied land-surface temperature. Clouds were removed using the QA60 band together with the s2cloudless probability layer, and per-pixel median composites were produced to suppress residual cloud and haze and to obtain gap-free imagery for each epoch.

From the composites, a feature stack was assembled comprising the visible, red-edge, near-infrared (NIR), and short-wave infrared (SWIR) bands, six spectral indices, and a Shuttle Radar Topography Mission (SRTM) elevation layer. The Normalised Difference Vegetation Index (NDVI) was computed to characterise vegetation vigour, as defined in (1).

$$NDVI = (\rho NIR - \rho Red) / (\rho NIR + \rho Red) \quad (1)$$

where ρNIR and ρRed are the surface reflectance of the near-infrared and red bands. Built-up land was emphasised through the Normalised Difference Built-up Index (NDBI), expressed in (2), while the Normalised Difference Water Index (NDWI), Enhanced Vegetation Index (EVI), Soil-Adjusted Vegetation Index (SAVI), and Bare-Soil Index (BSI) captured water bodies, dense canopy, sparse vegetation, and exposed soil, respectively.

$$NDBI = (\rho SWIR1 - \rho NIR) / (\rho SWIR1 + \rho NIR) \quad (2)$$

The full set of input features used to train the classifier is listed in Table 1.

Table 1. Input Features Used for the Random Forest Classification

Feature	Type	Description / role
B2, B3, B4	Spectral	Visible blue, green, red reflectance
B8 (NIR)	Spectral	Vegetation and water discrimination
B11, B12	Spectral	SWIR; soil and built-up separation
NDVI	Index	Vegetation vigour
NDWI	Index	Open-water detection
NDBI	Index	Built-up / impervious surface
EVI, SAVI	Index	Canopy density, sparse cover
BSI	Index	Bare-soil exposure
DEM	Topographic	SRTM elevation
LST	Climate	Land-surface temperature

Land-surface temperature was retrieved from the thermal infrared band of Landsat-8/9 Collection-2 Level-2 products, which provide atmospherically corrected surface temperature. The values were converted to degrees Celsius, cloud-masked using the pixel-quality band, and composited to the same dry-season windows as the optical data so that the thermal and spectral layers were temporally consistent. The resulting LST layer served both as an input feature for classification and as an independent variable for the climate analysis.

Reference samples for six land-cover classes—water body, forest or dense vegetation, cropland or agriculture, shrub and grassland, built-up area, and bare soil—were collected through stratified visual interpretation of high-resolution basemap imagery, yielding 1,240 labelled points. The samples were randomly partitioned into 70% for training and 30% for independent validation. Classification used the GEE implementation of Random Forest, ee.Classifier.smileRandomForest, with the number of trees and the number of variables sampled per split tuned through repeated trials; a configuration of 150 trees provided a stable balance between accuracy and computation.

Random Forest is an ensemble method that grows many decision trees on bootstrapped subsets of the training data, selecting a random subset of features at each node split and aggregating the individual tree votes by majority rule (Breiman, 2001). This randomisation decorrelates the trees and reduces variance, making the classifier resistant to overfitting and to correlated, high-dimensional inputs such as the spectral–index stack used here (Pal, 2005; Rodriguez-Galiano et al., 2012). Two hyper-parameters chiefly govern its behaviour: the number of trees, which stabilises predictions as it increases, and the number of variables considered per split, conventionally set near the square root of the total feature count. The algorithm also yields an out-of-bag error estimate and a variable-importance ranking based on the mean decrease in Gini impurity, the latter exploited in this study to interpret which features drive class separability.

Classifier performance was evaluated on the validation set using a confusion matrix, from which overall accuracy, producer accuracy, user accuracy, and the F1-score were derived. The kappa coefficient,

E-ISSN: 3123-2574
DOI: https://doi.org/10.64803/ikosstemi.v2.152 | Page: 18-24

which measures agreement corrected for chance, was computed as in (3).

$$\kappa = (p_o - p_e) / (1 - p_e) \qquad (3)$$

In these assessments, producer accuracy expresses the proportion of validation samples of a given class that were correctly mapped (a measure of omission error), whereas user accuracy expresses the proportion of pixels mapped as a class that truly belong to it (a measure of commission error). The F1-score, the harmonic mean of the two, provides a single balanced indicator per class, and overall accuracy summarises performance across all classes. Reporting this full set of metrics, rather than overall accuracy alone, prevents a high aggregate value from masking weak performance on individual or minority classes.

where p_o is the observed proportion of correctly classified samples and p_e is the expected agreement by chance. For comparison, Classification and Regression Tree (CART) and Support Vector Machine (SVM) classifiers were trained on the identical feature stack and sample split. Finally, class areas for 2019 and 2024 were tabulated, and the relationship between NDVI and LST was examined to link land-cover change with local surface warming.

III. RESULTS AND DISCUSSION

The Random Forest classifier produced a coherent land-cover map of the study area for 2024, shown in Figure 2. Cropland and agricultural land dominate the landscape, interspersed with patches of forest and shrub, while built-up land concentrates on the eastern bank of the main river corridor and water features are clearly delineated.

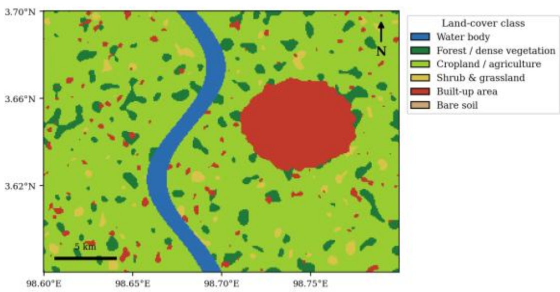

Source: Processed data, 2024

Figure 2. Random Forest land-cover classification of the Medan–Deli Serdang study area derived from Sentinel-2 imagery (2024).

Quantitative validation confirms the visual quality of the map. As summarised in Table 2, per-class F1-scores range from 0.86 for shrub and grassland—the class most often confused with cropland—to 0.97 for water bodies. Built-up areas were mapped with high reliability owing to the contribution of NDBI and the SWIR bands.

Table 2. Per-Class Accuracy of the Random Forest Classification

Land-cover class	PA (%)	UA (%)	F1
Water body	97.8	96.1	0.97
Forest / dense veg.	91.5	90.2	0.91
Cropland / agric.	93.0	94.4	0.94
Shrub & grassland	85.2	86.9	0.86
Built-up area	92.6	91.0	0.92
Bare soil	88.4	87.3	0.88

The detailed confusion matrix underlying these statistics is reported in Table 3. Most misclassification occurs between cropland and shrub or grassland, which share similar mid-season reflectance, and to a lesser extent between forest and cropland at field margins. Water, built-up, and bare-soil classes are well separated, reflecting their distinct spectral and thermal signatures.

Table 3. Confusion Matrix of the Random Forest Classification (Validation Samples)

Class (ref ↓ / pred →)	Wat	For	Crp	Shr	Bld	Bar	Total
Water	88	0	1	0	0	1	90
Forest	0	97	6	3	0	0	106
Cropland	1	5	133	8	3	3	153
Shrub	0	4	9	75	0	0	88
Built-up	0	0	3	0	63	2	68
Bare soil	1	0	3	0	3	61	68

Across all classes the RF model attained an overall accuracy of 92.4% and a kappa coefficient of 0.906, indicating almost-perfect agreement. When the same features and samples were supplied to the alternative classifiers, RF outperformed both SVM and CART, as reported in Table 4. The 4–6 percentage-point advantage is consistent with comparative findings in the literature (Thanh Noi & Kappas, 2018; Ouchra et al., 2024) and reflects the ability of the ensemble to model non-linear class boundaries without overfitting.

Table 4. Accuracy Comparison of the Tested Classifiers

Classifier	Overall accuracy (%)	Kappa
Random Forest	92.4	0.906

Support Vector Machine	88.7	0.857
Classification & Regression Tree	86.1	0.824

The variable-importance analysis in Figure 3 explains this performance. NDVI was the single most informative predictor, followed by the near-infrared band and NDWI, confirming that vegetation and moisture contrasts carry most of the discriminative signal. Land-surface temperature ranked fifth, demonstrating that the climate variable contributed meaningfully to separating impervious from vegetated surfaces rather than acting merely as auxiliary data.

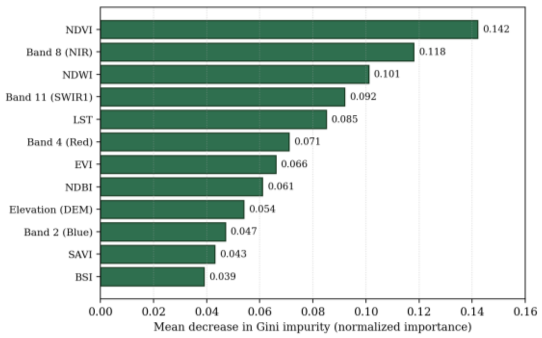

Source: Processed data, 2024

Figure 3. Random Forest variable importance based on the mean decrease in Gini impurity.

Multitemporal comparison reveals clear environmental change. Between 2019 and 2024 the built-up class expanded by 18.7%, while forest and cropland declined by 9.3% and 6.1%, respectively, as detailed in Table 5. The expansion is concentrated along transport corridors radiating from the urban core, a pattern typical of peri-urban sprawl in rapidly growing Indonesian cities.

Table 5. Land-Cover Area Change Between 2019 and 2024

Class	2019 (ha)	2024 (ha)	Change (%)
Built-up area	12,840	15,240	+18.7
Forest	21,360	19,380	−9.3
Cropland	48,720	45,760	−6.1
Shrub & grass	9,540	10,180	+6.7
Bare soil	3,210	4,060	+26.5

These land-cover dynamics have a direct climatic signature. Pixel-level comparison of NDVI and LST shows a strong negative correlation (r = −0.91), illustrated in Figure 4: areas that converted from vegetation to built-up surfaces between the two epochs recorded mean land-surface temperatures roughly 3 to 5 degrees Celsius higher than retained vegetated areas, while zones with NDVI below 0.4 consistently exhibited the highest surface temperatures. This inverse relationship corroborates evidence that vegetation loss amplifies surface heating and the urban heat-island effect, and it aligns with automated GEE studies that report random-forest models capturing strong non-linear links between vegetation cover and surface temperature. The integration of an explicit climate variable therefore allows the workflow to move beyond static mapping toward an interpretable indicator of environmental stress.

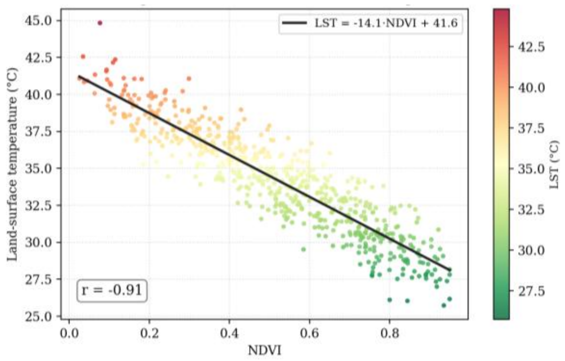

Source: Processed data, 2024

Figure 4. Relationship between NDVI and land-surface temperature across the study area, showing a strong negative correlation.

Compared with earlier work, the present study confirms the suitability of median compositing on GEE for producing accurate, cloud-free inputs (Phan et al., 2020) and reinforces the consistent superiority of RF over single-tree and margin-based classifiers for Sentinel-2 land cover. Its contribution lies in coupling this established mapping capability with change analysis and LST, yielding a monitoring product that is both accurate and policy-relevant. The principal limitation is the reliance on visually interpreted reference samples and a single dry-season window per year, which may underrepresent seasonal classes; incorporating field validation and multi-season composites would further strengthen the results.

The overall accuracy of 92.4% and kappa of 0.906 obtained here sit comfortably within the range reported for comparable Sentinel-2 studies on GEE. Thanh Noi and Kappas (2018) likewise found Random Forest to equal or exceed support-vector and nearest-neighbour classifiers on Sentinel-2 imagery, while specialised multitemporal workflows in more complex terrain have reached accuracies near 0.945

by aggregating many dates and textural features. That a comparatively lean single-season feature stack achieves accuracy in this band suggests that, for the relatively contrasted land cover of the Medan–Deli Serdang corridor, the marginal benefit of additional temporal layers is modest—an encouraging result for operational monitoring where processing economy matters. The agreement between the present benchmark and the wider literature also lends external credibility to the change and temperature statistics derived from the same classification.

IV. CONCLUSION

This study developed and validated a reproducible Google Earth Engine workflow that integrates multitemporal Sentinel-2 imagery, spectral indices, topography, and land-surface temperature with Random Forest classification for environmental and climate monitoring in North Sumatra. The main findings are: The Random Forest classifier achieved an overall accuracy of 92.4% and a kappa coefficient of 0.906, outperforming SVM (88.7%) and CART (86.1%) on identical inputs. NDVI, the near-infrared band, and NDWI were the most influential predictors, and the inclusion of land-surface temperature improved the separation of built-up from vegetated surfaces. Between 2019 and 2024 built-up land expanded by 18.7% while forest and cropland contracted, and this change coincided with a 3 to 5 degree Celsius rise in surface temperature over converted areas, confirming a strong inverse vegetation–temperature relationship. The GEE–RF approach offers a low-cost, scalable, and replicable basis for routine monitoring; its main weaknesses are dependence on visually interpreted samples and single-season imagery, which define clear avenues for refinement.

V. RECOMMENDATIONS

Future research should incorporate field-verified training samples and multi-season image composites to capture phenological variation and improve the separability of cropland, shrub, and grassland. Extending the time series beyond two epochs and adding Sentinel-1 radar data would enhance change detection under persistent cloud cover. Finally, coupling the classification output with hydrological and air-temperature models could translate the monitoring product into quantitative climate-risk indicators to directly support regional spatial planning.

VI. REFERENCES

Amani, M., Ghorbanian, A., Ahmadi, S. A., Kakooei, M., Moghimi, A., Mirmazloumi, S. M., Moghaddam, S. H. A., Mahdavi, S., Ghahremanloo, M., Parsian, S., Wu, Q., & Brisco, B. (2020). Google Earth Engine cloud computing platform for remote sensing big data applications: A comprehensive review. IEEE Journal of Selected Topics in Applied Earth Observations and Remote Sensing, 13, 5326–5350. https://doi.org/10.1109/JSTARS.2020.3021052

Belgiu, M., & Dragut, L. (2016). Random forest in remote sensing: A review of applications and future directions. ISPRS Journal of Photogrammetry and Remote Sensing, 114, 24–31. https://doi.org/10.1016/j.isprsjprs.2016.01.011

Breiman, L. (2001). Random forests. Machine Learning, 45(1), 5–32. https://doi.org/10.1023/A:1010933404324

Gorelick, N., Hancher, M., Dixon, M., Ilyushchenko, S., Thau, D., & Moore, R. (2017). Google Earth Engine: Planetary-scale geospatial analysis for everyone. Remote Sensing of Environment, 202, 18–27. https://doi.org/10.1016/j.rse.2017.06.031

Habibie, M. I. (2022). The application of machine learning using Google Earth Engine for remote sensing analysis. Jurnal Teknoinfo, 16(2), 233. https://doi.org/10.33365/jti.v16i2.1872

Ouchra, H., Belangour, A., & Erraissi, A. (2024). Supervised machine learning algorithms for land cover classification in Casablanca, Morocco. Ingenierie des Systemes d Information, 29(1), 377–387. https://doi.org/10.18280/isi.290137

Pal, M. (2005). Random forest classifier for remote sensing classification. International Journal of Remote Sensing, 26(1), 217–222. https://doi.org/10.1080/01431160412331269698

Phan, T. N., Kuch, V., & Lehnert, L. W. (2020). Land cover classification using Google Earth Engine and random forest classifier—The role of image composition. Remote Sensing, 12(15), 2411. https://doi.org/10.3390/rs12152411

Rodriguez-Galiano, V. F., Ghimire, B., Rogan, J., Chica-Olmo, M., & Rigol-Sanchez, J. P. (2012). An assessment of the effectiveness of a random forest classifier for land-cover classification. ISPRS Journal of Photogrammetry and Remote Sensing, 67, 93–

104. https://doi.org/10.1016/j.isprsjprs.2011.11.002

Supiyandi and R. b. Mailok, "Urban Vegetation Cover Prediction Model Using Google Earth Engine Based on NDVI Sentinel-2 in Batu Bara Regency, Indonesia," 2025 International Conference on Computing and Applied Informatics (ICCAI), Medan, Indonesia, 2025, pp. 1-7, https://doi.org/10.1109/ICCAI65301.2025.11278944

Talukdar, S., Singha, P., Mahato, S., Shahfahad, Pal, S., Liou, Y.-A., & Rahman, A. (2020). Land-use land-cover classification by machine learning classifiers for satellite observations—A review. Remote Sensing, 12(7), 1135. https://doi.org/10.3390/rs12071135

Tamiminia, H., Salehi, B., Mahdianpari, M., Quackenbush, L., Adeli, S., & Brisco, B. (2020). Google Earth Engine for geo-big data applications: A meta-analysis and systematic review. ISPRS Journal of Photogrammetry and Remote Sensing, 164, 152–170. https://doi.org/10.1016/j.isprsjprs.2020.04.001

Tassi, A., & Vizzari, M. (2020). Object-oriented LULC classification in Google Earth Engine combining SNIC, GLCM, and machine learning algorithms. Remote Sensing, 12(22), 3776. https://doi.org/10.3390/rs12223776

Thanh Noi, P., & Kappas, M. (2018). Comparison of random forest, k-nearest neighbor, and support vector machine classifiers for land cover classification using Sentinel-2 imagery. Sensors, 18(1), 18. https://doi.org/10.3390/s18010018